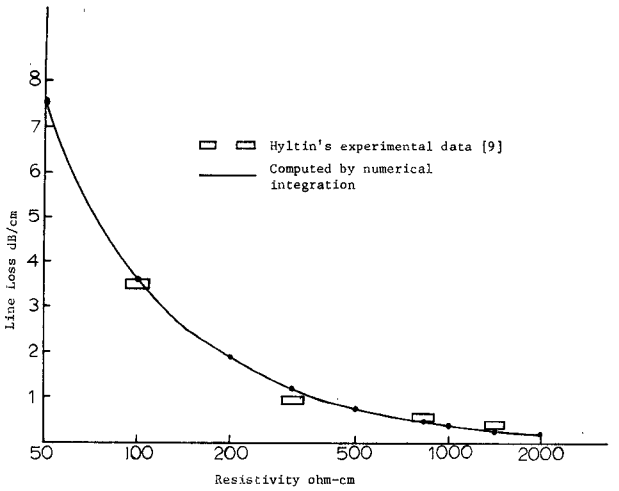

Fig. 4. Microstrip line loss versus resistivity of the dielectric substrates. $\epsilon_r = 11.7$.

the point (x_1,y_1,z_1) is on this plane.

Let

$$\boldsymbol{P}\cdot\boldsymbol{N} = C_1.$$

Then

$$\boldsymbol{R}\cdot\boldsymbol{N} = C_1$$

or

$$xN_x + yN_y + zN_z = C_1$$

$$z(x,y) = \Phi(x,y) = \frac{C_1 - xN_x - yN_y}{N_z}$$

$$\boldsymbol{E} = -\frac{\partial\Phi}{\partial x}\hat{a}_x - \frac{\partial\Phi}{\partial y}\hat{a}_y$$

$$= \frac{N_x}{N_z}\hat{a}_x + \frac{N_y}{N_z}\hat{a}_y$$

$$|E|^2 = \frac{N_x^2 + N_y^2}{N_z^2}.$$

REFERENCES

[1] R. A. Pucell, D. J. Massé, and C. P. Hartwig, "Losses in microstrip," *IEEE Trans. Microwave Theory Tech.*, vol. MTT-16, pp. 342–350, June 1968.
[2] M. V. Schneider, "Microstrip lines for microwave integrated circuits," *Bell Syst. Tech. J.*, vol. 48, pp. 1421–1444, May–June 1969.
[3] R. Horton, B. Easter, and A. Gopinath, "Variation of microstrip losses with thickness of strip," *Electron. Lett.*, vol. 7, pp. 490–491, Aug. 26, 1971.
[4] M. V. Schneider, "Dielectric loss in integrated microwave circuits," *Bell Syst. Tech. J.*, vol. 48, pp. 2325–2332, Sept. 1969.
[5] J. D. Welch and H. J. Pratt, "Losses in microstrip transmission systems for integrated microwave circuits," *NEREM Rec.*, vol. 8, pp. 100–101, Nov. 1966.
[6] M. Caulton, J. J. Hughes, and H. Sobol, "Measurement of the properties of microstrip transmission lines for microwave integrated circuits," *RCA Rev.*, vol. 27, pp. 377–391, Sept. 1966.
[7] A Farrar and A. T. Adams, "Characteristic impedance of microstrip by the method of moments," *IEEE Trans. Microwave Theory Tech.*, (Corresp.), vol. MTT-18, pp. 65–66, Jan. 1970.
[8] A. Gopinath and B. Easter, "Moment method of calculating discontinuity inductance of microstrip right-angled bends," *IEEE Trans. Microwave Theory Tech.* (Short Papers), vol. MTT-22, pp. 880–883, Oct. 1974.
[9] T. M. Hyltin, "Microstrip transmission on semiconductor dielectrics," *IEEE Trans. Microwave Theory Tech.* (1965 Symposium Issue), vol. MTT-13, pp. 777–781, Nov. 1965.

The Electric-Dipole Resonances of Ring Resonators of Very High Permittivity

M. VERPLANKEN AND J. VAN BLADEL, FELLOW, IEEE

***Abstract*—The lowest confined mode in a coaxial ring resonator is investigated. Data are given about the Q of the mode, the eigen-electric dipole at resonance, and the structure of the electric field surrounding the resonator. The data are valid for high, but finite values of ϵ_r.**

I. INTRODUCTION

In a previous paper [1], Van Bladel has shown that a dielectric body of revolution [Fig. 1(a)] admits, in the limit $\epsilon_r = N^2 \to \infty$, a resonant mode of the form

$$\bar{H}_m = \beta_m(r,z)\bar{u}_\phi \tag{1}$$

where β_m satisfies

$$\frac{\partial^2\beta_m}{\partial r^2} + \frac{1}{r}\frac{\partial\beta_m}{\partial r} + \frac{\partial^2\beta_m}{\partial z^2} - \frac{\beta_m}{r^2} + k_m^2\beta_m = 0 \quad \text{in} \quad S. \tag{2}$$

In addition, β_m vanishes on the outer contour (c) and on the z axis. The mode under discussion is a *confined mode*, which means that it takes the value (1) in the dielectric, but vanishes outside S. For such a case the boundary surface acts as a magnetic wall. When N is finite but large, the mode is found to radiate like an electric dipole of moment $\bar{p}_e$. As a result, energy is lost by radiation, and a finite Q affects the resonance. The value of Q is proportional with N^5, while it is proportional with N^3 for a magnetic-dipole mode. The strong increase of Q with N is the reason why the electric-dipole mode is of interest for applications. We proceed to calculate $\bar{p}_e$ and Q for the ring resonator shown in Fig. 1(b). The limit form $b = 0$ corresponds to a circular cylinder, a structure which is often used in practice.

II. FORMULAS FOR DIPOLE MOMENT AND Q

The determination of these quantities requires solution of the following exterior potential problem [1]

$$\nabla^2\phi = 0 \quad \text{outside} \quad S$$

Manuscript received April 14, 1975, revised July 14, 1975.
The authors are with the Laboratory for Electromagnetism and Acoustics, University of Ghent, B-900 Ghent, Belgium.

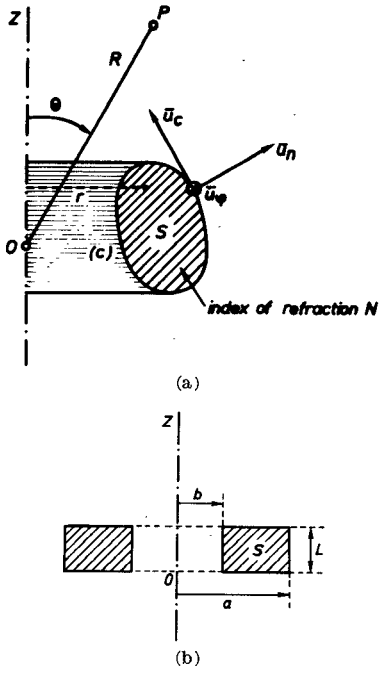

Fig. 1. (a) Dielectric resonator with symmetry of revolution. (b) Coaxial ring resonator.

$$\frac{\partial \phi}{\partial c} = \frac{R_c}{jk_m}\frac{\partial \beta_m}{\partial n} \quad \text{on} \quad (c) \tag{3}$$

$$\iint_{S_w} \frac{\partial \phi}{\partial n}\, dS = 0,$$

$$\phi = A\frac{\cos\theta}{R^2} \quad \text{at large distances}$$

$$\phi = 0 \quad \text{on the } z \text{ axis.}$$

As ϕ depends only on r and z, the first equation takes the form

$$\frac{\partial^2 \phi}{\partial r^2} + \frac{1}{r}\frac{\partial \phi}{\partial r} + \frac{\partial^2 \phi}{\partial z^2} = 0. \tag{4}$$

The second condition, where R_c is the characteristic impedance of free space, expresses continuity of the tangential electric field on (c). The third condition, where the integral is over the ring boundary surface S_w, expresses charge neutrality. The fourth condition, where A is a still undetermined factor, implies that ϕ is the potential created by an electric dipole. The sought quantities, $\bar{p}_e$ and Q, are given in terms of ϕ by

$$\bar{p}_e = \frac{\epsilon_0}{N}\left[\iint_{S_w} \frac{\partial \phi}{\partial n}\bar{r}\, dS - \iint_{S_w} \phi \bar{u}_n\, dS\right] \tag{5}$$

$$\iint \beta^2 r\, dS$$

$$Q = \frac{12\pi^2 N^3}{k_m^3 c^2}\frac{S}{|\bar{p}_e|^2}. \tag{6}$$

III. FORMULATION OF THE RING-RESONATOR PROBLEM

With reference to the geometry of Fig. 1(b), the general solution for β is of the form

$$\beta_{ns} = B_{ns}\sin\frac{n\pi z}{L}R_n\left(x_{ns}\frac{r}{a}\right), \qquad (B_{ns} \text{ in } \mathrm{A\cdot m^{-1}}) \tag{7}$$

where R_n is a solution of Bessel's equation. We write R_n as

$$R_n(z) = J_n(z) + C_{ns}Y_n(z). \tag{8}$$

The parameter x is quantized by the boundary conditions

$$R_n(x_{ns}) = 0, \qquad (\text{condition } \beta = 0 \text{ for } r = a)$$

$$R_n\left(\frac{b}{a}x_{ns}\right) = 0, \qquad (\text{condition } \beta = 0 \text{ for } r = b) \tag{9}$$

and the resonant wavenumber follows from

$$k_{ns}^2 = \left(\frac{n\pi}{L}\right)^2 + \left(\frac{x_{ns}}{a}\right)^2. \tag{10}$$

We shall concentrate our attention on the lowest $n = 1$ mode. Here, x is determined by the condition

$$\frac{J_1(x_{11})}{Y_1(x_{11})} = \frac{J_1\left(\frac{b}{a}x_{11}\right)}{Y_1\left(\frac{b}{a}x_{11}\right)}. \tag{11}$$

The roots of this "coaxial-line" type of secular equation are well known [2]. Some of them are given in Table I, together with C_{11}, and the value of B_{11} which gives a maximum value of $+1$ $\mathrm{A\cdot m^{-1}}$ for β_{11} (i.e., for $B_{11}R_1$) in the dielectric cross section S. The Neumann function Y_1 is defined as in [3].

A sketch of the variation of x_{11} with b/a is shown on Fig 2. The boundary conditions of the differential problem are specifically (Fig. 3):

1) in A and to the right of A (along the $z = L/2$ axis), $\phi = 0$;
2) between A and B

$$\phi = jR_cB_{11}\frac{Lx_{11}}{k_{11}a}\cos\frac{\pi z}{L}R_0(x_{11})$$

where

$$R_0(z) = J_0(z) + C_{11}Y_0(z)$$

TABLE I

b/a	x_{11}	C_{11}	B_{11} ($\mathrm{A\cdot m^{-1}}$)
0	3.8317	0	1.7185
0.25	4.4475	0.6887	1.665
0.50	6.3932	-0.7099	-2.208
0.75	12.6056	-0.8709	-3.131

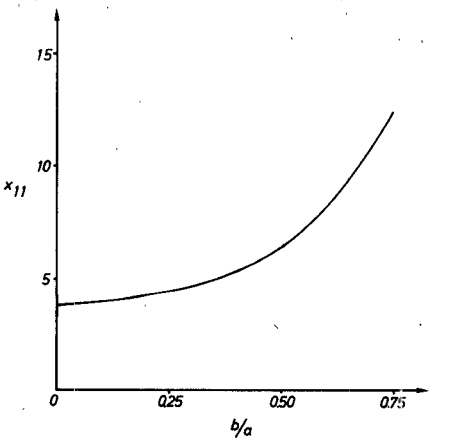

Fig. 2. Plot of the quantized parameter x_{11}, as introduced in (11).

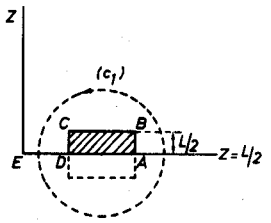

Fig. 3. Relevant to the definition of the differential problem.

3) between B and C

$$\phi = jR_cB_{11}\left[\frac{\pi a}{k_{11}x_{11}L}R_0\left(x_{11}\frac{r}{a}\right) - \frac{k_{11}La}{\pi x_{11}}R_0(x_{11})\right]$$

4) between D and C

$$\phi = jR_cB_{11}\frac{x_{11}L}{\pi k_{11}a}\cos\frac{\pi z}{L}R_0\left(x_{11}\frac{b}{a}\right) + jR_cB_{11}\frac{k_{11}La}{\pi x_{11}}\left[R_0\left(x_{11}\frac{b}{a}\right) - R_0(x_{11})\right]$$

5) in D, and between D and E

$$\phi = jR_cB_{11}\frac{k_{11}La}{\pi x_{11}}\left[R_0\left(x_{11}\frac{b}{a}\right) - R_0(x_{11})\right].$$

The potential ϕ generates the external electric field through the formula

$$\bar{E} = \frac{1}{N}\operatorname{grad}\phi. \tag{12}$$

This value holds in the "near" region, i.e., up to distances small compared with the wavelength in free space, which is

$$\lambda_0 = N\lambda_{\text{diel}} = N\frac{2\pi}{k_{11}} = N\frac{2\pi}{\left[\left(\frac{\pi}{L}\right)^2 + \left(\frac{x_{11}}{a}\right)^2\right]^{1/2}}. \tag{13}$$

It is to be noticed that ϕ is multiple valued, as curl $\bar{E}$ is zero outside the dielectric, but different from zero inside. As a result, $\int\bar{E}\cdot\overline{dl} \neq 0$ for a curve surrounding the dielectric (such as C_1 in Fig. 3). This is the reason why ϕ has different values in A and D.

IV. NUMERICAL RESULTS

After consideration of several methods, we decided to solve the differential problem (3) by finite differences, as the shape of the boundary is particularly suitable for the purpose [4]. The matrix problem was solved by successive overrelaxation methods [5]. The boundary condition at large distances was applied in the form "ϕ proportional with $\cos\theta/R^2$" as shown in (3). One could replace this condition by the requirement that ϕ vanish along a large circle (of radius $R = 10a$ for example). It was found that this step was too drastic and resulted in poor convergence. The potential at large distances is related to the electric moment by

$$\phi = A\frac{\cos\theta}{R^2} = -\frac{p_e\cos\theta}{4\pi\epsilon_0R^2}. \tag{14}$$

The sought value of p_e can therefore be obtained either by observing the behavior of ϕ at large distances [and deducing p_e from (14)], or by taking the values of ϕ and $\partial\phi/\partial n$ at the dielectric boundary into account, as in (5). It was found that the second method gave considerably better results for a given net size, provided the values of $\partial\phi/\partial n$ were evaluated by carefully selected interpolation methods (such as Newton's $\frac{3}{8}$ rule, combined with Simpson's rule). Some of the more interesting numerical results are shown in Figs. 4–6. In Fig. 4 we have shown the potential distribution for two typical geometries. The plotted function is not the potential itself, but the dimensionless expression

$$\tau\left(\frac{r}{a}, \frac{z}{a}, \frac{b}{a}, \frac{L}{a}\right) = \frac{\phi_{\text{norm}}}{jR_ca\cdot(1\ \text{A}\cdot\text{m}^{-1})} \tag{15}$$

where ϕ_{norm} is the potential associated with the normed eigenfunction, i.e., with the value of B_{11} appearing in Table I. The value of the potential for an arbitrary B_{11} is then simply

$$\phi = \frac{B_{11}}{(B_{11})_{\text{norm}}}jR_ca\tau.$$

ϕ is in volts, R_c in ohms, a in meters, and τ is the number read from Fig. 4. The full lines represent the equipotential lines. The dashed lines are the equipotentials of the dipole moment $\bar{p}_e$, assumed con-

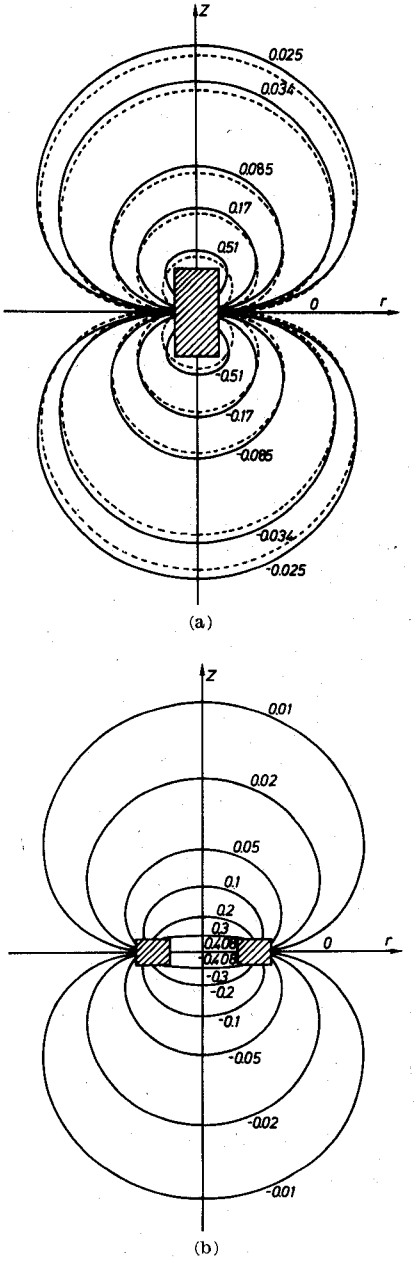

Fig. 4. Potential distribution for two particular geometries.

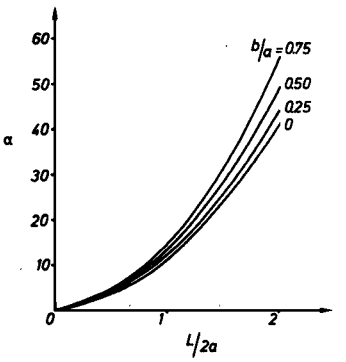

Fig. 5. Plot of the dimensionless factor α, as introduced in (16).

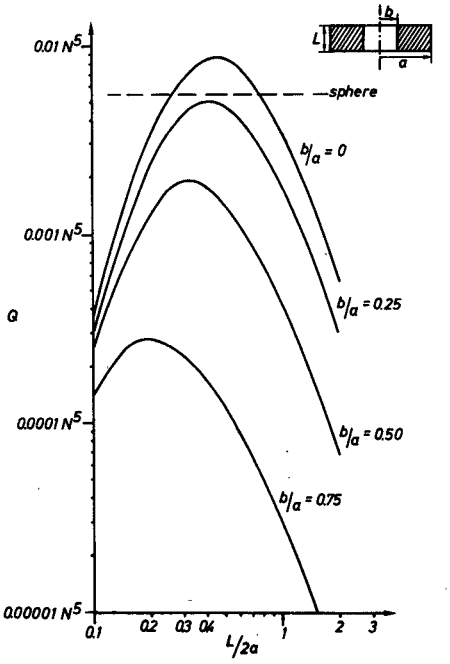

Fig. 6. Q factor of the ring resonator.

centrated at the center of the resonator. Both equipotentials tend to coincide at large distances.

Inserting τ in (5) allows one to write $\bar{p}_e$ in the form

$$\bar{p}_e = -\frac{ja^3}{Nc}\left[\iint_{s_w}\left(\tau\bar{u}_n - \frac{\partial\tau}{\partial(n/a)}\frac{\bar{r}}{a}\right)\frac{dS}{a^2}\right] \times (1\ \mathrm{A\cdot m^{-1}}). \quad (16)$$

Here again, $\bar{p}_e$ is the value corresponding to the normed eigenfunction. The quantity between brackets is dimensionless, and is a function of b/a and $L/2a$. It will be denoted by $\alpha\bar{u}_z$, and its magnitude is plotted in Fig. 5. The dipole moment for an arbitrary value of B_{11} is

$$\bar{p}_e = -\frac{ja^3}{Nc}\alpha\bar{u}_z\frac{B_{11}}{(B_{11})_{\mathrm{norm}}}.$$

$\bar{p}_e$ is in $\mathrm{C\cdot m^{-1}}$, a in meters, and c in $\mathrm{m\cdot s^{-1}}$.

From the knowledge of $\bar{p}_e$ it is a simple matter to determine Q through (6). The results are shown in Fig. 6. For comparison, we have shown the Q factor of a sphere of radius a, resonating in the lowest ϕ-independent confined mode

$$\bar{H}_m = \sin\theta\left(\frac{\sin kR}{R^2} - k\frac{\cos kR}{R}\right)\bar{u}_\phi \quad (17)$$

where $ka = 4.49$.

V. SAMPLE CALCULATION

We wish to utilize a material of $\epsilon_r = 144$ to design a resonator which resonates at 1500 MHz and has optimum Q. We also wish to investigate the value of the induced fields and $\bar{p}_e$ at resonance when the resonator is illuminated with a plane wave of electric field parallel with the axis of the resonator.

A look at Fig. 6 shows that maximum Q is obtained for $b/a = 0$ (i.e., for a circular cylinder), and $L/2a = 0.45$. The value of Q is $0.0086N^5 = 2140$. The wavelength in the dielectric is

$$\lambda_{\mathrm{diel}} = \frac{\lambda_0}{N} = \frac{20\ \mathrm{cm}}{12} = 1.66\ \mathrm{cm}.$$

The dimensions can now be derived from (10), i.e., from the relationship

$$k_{11}^2 = \left(\frac{\pi}{L}\right)^2 + \left(\frac{3.8317}{a}\right)^2 = \left(\frac{2\pi}{\lambda_{\mathrm{diel}}}\right)^2.$$

This gives $a = 1.375$ cm and $L = 1.238$ cm. The induced dipole moment at resonance is [6]

$$\bar{P}_e = -j\frac{6\pi N^3\epsilon_0}{(k_{11})^3}\bar{E}_i = -j\,5.3\ 10^{-15}\bar{E}_i \quad \mathrm{C\cdot m}$$

where $\bar{E}_i$ is the incident electric field in $V \cdot m^{-1}$. The induced magnetic field in the resonator is, again at resonance [6],

$$\bar{H} = -\frac{\bar{P}_e \cdot \bar{p}_e}{|\bar{p}_e|^2} (B_{11})_{\text{norm}} \sin\frac{\pi z}{L} R_1\left(x_{11}\frac{r}{a}\right)\bar{u}_\phi$$

$$= 3.96 \sin\frac{\pi z}{L} J_1\left(3.8317\frac{r}{a}\right) E_i \bar{u}_\phi$$

as $\bar{p}_e = -j(a^3/Nc)\alpha\bar{u}_z$. The value of α, read off on Fig. 6, is 3.14.

REFERENCES

[1] J. Van Bladel, "On the resonances of a dielectric resonator of very high permittivity," *IEEE Trans. Microwave Theory Tech.*, vol. MTT-23, pp. 199–208. Feb. 1975.

[2] C. G. Montgomery, *Technique of Microwave Measurements*. New York: McGraw-Hill, 1947, p. 305.

[3] M. Abramowitz and I. Stegun, *Handbook of Mathematical Tables*. New York: Dover, 1965.

[4] For more details concerning numerical procedures, see M. Verplanken's Ph.D. thesis (in preparation).

[5] J. Westlake, *A Handbook of Numerical Matrix Inversion and Solution of Linear Equations*. New York: Wiley, 1968.

[6] J. Van Bladel, "The excitation of dielectric resonators of very high permittivity," *IEEE Trans. Microwave Theory Tech.*, vol. MTT-23, pp. 208–217, Feb. 1975.

Resonant Frequency of a $TE_{01\delta}$° Dielectric Resonator

YOSHIHIRO KONISHI, NORIO HOSHINO, AND YOZO UTSUMI

***Abstract*—The resonant frequency of a $TE_{01\delta}$° dielectric resonator was obtained by assuming a cylindrical surface containing the circumference of a dielectric resonator as a magnetic wall. In such a method, the error was less than 10 percent. In this short paper, the resonant frequency is obtained by a variational method, where the surface impedance is variated from a infinite value [1]. The theoretical value of a resonant frequency has a good agreement with our experimental result with an error less than 1 percent.**

I. INTRODUCTION

In the past, the resonant frequency of a dielectric resonator was obtained by assuming a cylindrical surface containing the circumference of a dielectric resonator as a magnetic wall [2], and with this method error was less than 10 percent between the theoretical values and the experimental ones.

Yee [3] obtained the modified open-circuit boundary (OCB) approximation method for TE_{lm0}° mode but he assumed a cylindrical surface as a magnetic wall, and he obtained the variational method for TM_{1mn} mode, but he assumed two flat surfaces as a magnetic wall.

In our method, however, we do not assume only a cylindrical surface but also two flat surfaces as a magnetic wall. We assume the exponential decay in the z direction, and variate the surface impedance from a infinite value.

Manuscript received May 5, 1975; revised August 5, 1975.

The authors are with the NHK Technical Research Laboratories, Tokyo 157, Japan.

In the case where the sectional areas of a cylindrical dielectric resonator face the metal plates at a short distance as shown in Fig. 1(a) (as in the case of microwave integrated circuit (MIC) use, for example), the assumption of a magnetic wall mentioned before is quite reasonable because the RF field of the resonator is in parallel to the metal plates and crosses the cylindrical surface almost vertically. However, in the case where the resonator is placed in a free space or the distance between the resonator and the metal plates becomes large, the parallel component of the RF field approaches the axis of a resonator. This does not satisfy a magnetic wall assumption. The situation is shown in Fig. 1(b).

II. THEORETICAL VALUES BY MAGNETIC WALL APPROXIMATION

When assuming the surface S_0 to be a magnetic wall as shown in Fig. 2, the resonant frequency can be obtained from (1)

$$k_z \cdot \tan(k_z l/2) = \alpha \quad J_0(k_\rho a) = 0$$

$$k_\rho^2 + k_z^2 = \epsilon_r k_0^2 \quad k_\rho^2 - \alpha^2 = k_0^2$$

$$k_0 = \omega_0(\epsilon_0\mu_0)^{1/2} \quad x_0 = 2\pi a/\lambda \quad \xi = l/2a \tag{1}$$

where k_z is a propagation constant in a dielectric region along the z axis, α is a damping constant in an air region inside a space surrounded by S_0 along the axis, k_ρ is a wavenumber along a radius, and k_0 is a free-space wavenumber.

III. THEORETICAL VALUES OBTAINED BY A VARIATIONAL METHOD

We assume the trial scalar functions internal to S_0 to be ϕ_{1d} and ϕ_{1a}

$$\phi_{1d} = J_0(k_\rho\rho)\cos(k_z z) \qquad \text{(in dielectric)}$$

$$\phi_{1a} = \exp(\alpha l/2)\cos[k_z(l/2)]J_0(k_\rho\rho)\exp(-\alpha|z|) \qquad \text{(in air)}. \tag{2}$$

In this case, the wall admittance Y_ρ can be expressed by (3) using the scalar function of (2)

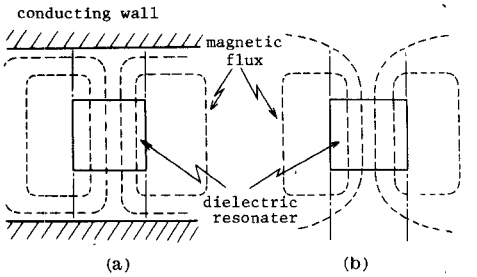

Fig. 1. Magnetic flux for $TE_{01\delta}$° mode. (a) Near the conducting wall. (b) In free space.

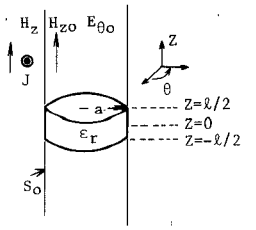

Fig. 2. Cylindrical coordinate system for dielectric cylinder.